Finite Array Decomposition Domain Method applied to large low profile metasurface-based antenna

Céline Ha, Jean-François Pintos, Priscillia Daquin, Serge Bories

Finite Array Decomposition Domain Method applied to large low profile metasurface-based antenna

Céline Ha[1], Jean-François Pintos[1], Priscillia Daquin[2], Serge Bories[1]
[1] Univ. Grenoble Alpes, CEA, Leti, F-38000 Grenoble, France
[2] CNES, Toulouse, France
celine.ha@cea.fr

***Abstract*— This paper examines the accuracy, the time and memory consumption of the Finite Array Domain Decomposition Method (FA-DDM) applied for a large and complex low-profile metasurface-based antenna, with High-Performance Computing (HPC) for parallel processing. A validation step is performed as the technique is used for non-identical unit cells in the lattice array. Three canonical and simple structures are simulated for validation: the half-wave dipole, the half-wave dipole over a Perfect Electric Conductor (PEC) and the half-wave flat dipole over a mushroom-like Artificial Magnetic Conductor (AMC). To conclude, a large antenna system (9 x 19 cells) with high complexity is proposed to investigate the performance of the FA-DDM.**

***Index Terms*— low-profile antenna, metasurface, AMC, HFSS, finite array, DDM design methodology.**

I. Introduction

Metasurfaces are 2D planar arrays of subwavelength metallic or dielectric structures, able to manipulate the incoming electromagnetic waves to achieve numerous electromagnetic operations: power absorption, focusing, wavefront tailoring, propagating surface waves suppression, in-phase full reflection of incident plane waves, etc. [1]-[3]. When a metasurface can perform the latter operation, it is designated Artificial Magnetic Conductor (AMC) as it behaves like a Perfect Magnetic Conductor (PMC) inside a narrow operating bandwidth. At the interface of a PMC, there is no phase shift between the primary field and the image field. Therefore, in the case of a parallel radiator over an AMC, it is advantageous to bring the radiator closer to the AMC in order to minimize the optical path length, and thus, to have constructive interferences. The overall structure is called low-profile antenna, for which its thickness is smaller compared to the wavelength ($< \lambda_0/10$).

Prototyping an efficient AMC is challenging as many parameters are involved in designing the unit cell, such as the geometry [4][5], the materials [6] or the use of lumped-elements and his circuitry for active AMC [7][8]. The behavior of the AMC is inferred by using periodic boundary conditions to simulate infinite large array under plane wave excitation. However, in the case of a low-profile metasurface-based antenna, an AMC is located in the near field of the radiator, leading to mutual interactions between these two elements (the metasurface and the radiator), and there are edge effects due to the AMC finite size. So far, as the condition of study of each individual component does not correspond to the real configuration of a low-profile antenna, it is necessary to use a commercial full-wave simulator to design and to optimize this antenna. However, by increasing the complexity and the number of cells forming the AMC, it will consume much computational time and memory, and in the worst case, cannot be solved.

Exposed issues are tackled in designing finite large arrays. In [9], the authors studied a complex array of helix antennas around a Teflon cylindrical support, operating at 8 GHz and 8.4 GHz. They have compared three different simulation techniques available in the commercial 3D electromagnetic software ANSYS HFSS [10]: the finite element method (FEM) or full-wave simulation for the explicit design, the infinite array simulation with periodic boundary conditions and Finite Array Domain Decomposition Method (FA-DDM). DDM takes advantage of the periodicity of the model by meshing a single unit cell and by repeating it along the array lattice to model the entire finite sized array domain. The results of their study show that FA-DDM running on 4 Central Processing Unit (CPU) cores spends less simulation time in meshing compared with FEM running on 2 CPU cores: 25.4% against 88.9% for a 3x3 cells array. Better accuracy for the S_{11} value is obtained with FA-DDM than infinite array simulation from 5x5 array size: 0.45% error against 20.7% at 8 GHz, and 16.6% error against 33.7% at 8.4 GHz. FA-DDM is also employed in [11] to evaluate computational statics when analyzing a 20 x 20 Frequency Selective Surface (FSS). The unit cell is a metallic cross placed between two dielectric substrates and plane wave excitation is applied. FA-DDM shows less time and memory consumption than full-wave simulation, with less CPU cores: full-wave simulation running on 12 cores with FEKO software requires 16.9 GB and spends 3298 CPU time/s, whereas FA-DDM running on 8 cores with HFSS software requires only 1.6 GB and spends 936 CPU time/s.

In [9] and [11], FA-DDM is used for symmetrical and similar structures, that is, with a unique unit cell. In this paper, the FA-DDM is extended to an unconventional model, the metasurface-based antenna. Thus, non-identical unit cells are created for regions where the radiator is over the metasurface (more details on cells will be presented in section IV.C). Time, memory consumption and accuracy between full-wave and FA-DDM techniques are compared for simple to complex structures: half-wave dipole alone and over a Perfect Electric Conductor (PEC), half-wave flat dipole over an AMC with mushroom-like unit cell and half-wave flat dipole over a large complex AMC. Simulations were performed with HFSS v2020R1.

II. Finite Array Domain Decomposition Method (FA-DDM)

The original model is decomposed into non-overlapping sub-domains, with non-conformal mesh interfaces between the unit cells. For a periodic array structure, a single unit cell is meshed and repeated to create the entire finite array. The initial problem, that is, solving a linear matrix equation, is adjusted to sub-domain problems with local solutions depending on the unit cell location and orientation in the array. As sub-domain problems can be solved in parallel, DDM allows operating simulations on distributed memory architecture, saving computational memory [12][13].

To use FA-DDM for non-periodic structures in HFSS, it is necessary to design each unit cells as a 3D Component, to define appropriated master/slave boundaries on the outer walls of the unit cell, and to preserve equal dimension between each unit cells. When creating a 3D Component array and arranging the unit cells in the array, it is possible to rotate the cells by 90° steps and thus, saving conception time for identical unit cells [13].

III. Setup

Simulations are performed with a discrete frequency sweep, automatic meshing, a ΔS of 0.02 for convergence and two minimum converged passes to stop the adaptive analysis. High-Performance Computing (HPC) is employed for parallel processing on multiple cores. The hardware used in the analysis consists of a cluster composed of two nodes; each node has 20 cores Xeon Gold 6148 at 2.4 GHz and 384 GB Random Access Memory (RAM). For full-wave simulation, solved frequencies are distributed in parallel over M selected cores. Meanwhile, for DDM, only one frequency is solved in parallel over M selected cores.

IV. 3D Simulations

Before considering a large electromagnetic problem, a validation phase is performed on three canonical and simple models: a half-wave dipole alone and over a PEC, and a flat half-wave dipole over a finite mushroom-like AMC.

A. Half-wave dipole validation

A cylindrical half-wave dipole operating a 1 GHz ($\lambda_0 = 300$ mm) is designed. The length of the dipole is $l = 140$ mm and its radius is $r = 1$ mm. A virtual excitation is applied at the center of the dipole in both simulations between the two arms. For DDM simulation, the dipole is sliced in three similar regions. The unit cell base is a square of 100 mm ($\lambda_0/3$) edge, Fig. 1. One padding cell is implemented to space the radiating element from the radiation boundary, that is, there is one unit cell distance of vacuum between each side of the array and the radiation boundary.

Z and S-parameters, Fig. 2, are obtained with a minimum of 5 passes in FEM simulation and a minimum of 10 passes in DDM simulation for the adaptive meshing step. The results in Table I are determined for 61 frequency points. DDM simulation requires a large number of mesh elements in order to match the results of a full-wave simulation, Table I. Distributed memory setup is oversized to study the half-wave dipole for both methods, as shown by simulation time and memory consumption. This first case is for validation only and it is not a practical use case.

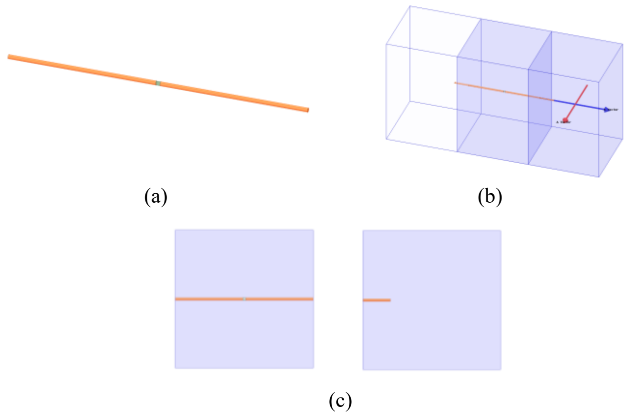

Fig. 1. Half-wave dipole in HFSS. (a) Full-wave method. (b) DDM. (c) 3D Component unit cells: a feeding part and an edge part.

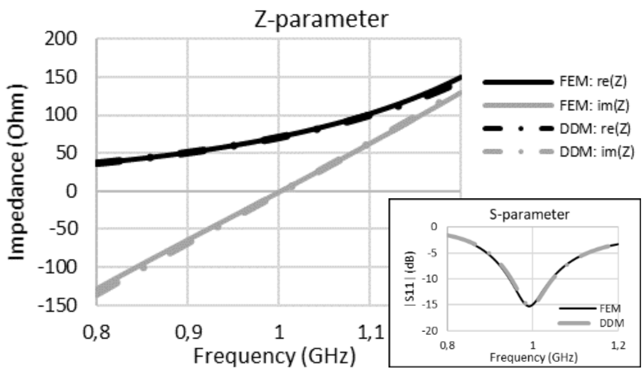

Fig. 2. Real and imaginary part of Z-parameter solved with FEM and DDM, and (inset) Magnitude of the reflection coefficient $|S_{11}|$, for a half-wave dipole.

TABLE I. Computational Performance for a Half-Wave Dipole

Method	*Unknowns*	*Adaptive Meshing (Time / Memory)*	*Frequency Sweep (Time / Memory)*
FEM	18 822	49 s / 2.19 GB	5 min 39 s / 14.05 GB
DDM	392 985	6 min 52 s / 15.04 GB	3 h32 min / 15.66 GB

B. *Half-wave dipole over a finite PEC validation*

The previous half-wave dipole is centered over a finite PEC at the height of h = 75 mm ($\lambda_0/4$), Fig. 3. The PEC size is 500 x 500 mm², which is 5x5 unit cells. About the design for the DDM simulation, in each unit cell, vacuum boxes of different height are nested in each others in order to improve the mesh in free space. Furthermore, maximum element length is set to $\lambda_0/25$ for the smallest nested box containing the dipole, which height is $\lambda_0/10$. One padding cell is implemented all around the PEC.

Z and S-parameters, Fig. 4, are obtained with a minimum of 5 passes in for both simulations. The results in Table II are determined for 61 frequency points. As with the case of the half-wave dipole alone, DDM simulation requires a large number of mesh elements in order to correspond to the results of a full-wave simulation. Even if HPC is oversized for this case of study, the memory consumption is reduced by 3.9 times during frequency sweep process with DDM, but with high cost in simulation time, 32 times higher than FEM simulation. This second case is also for validation only and it is not a practical use case.

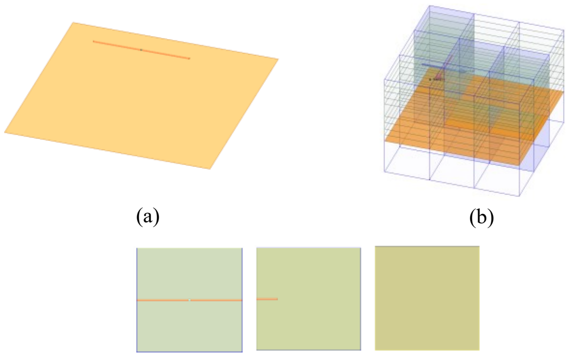

Fig. 3. Half-wave dipole over a finite PEC in HFSS. (a) Full-wave method. (b) DDM. (c) 3D Component unit cells: a feeding part over the ground plane, an edge part of the dipole over the ground plane and a part of the ground plane.

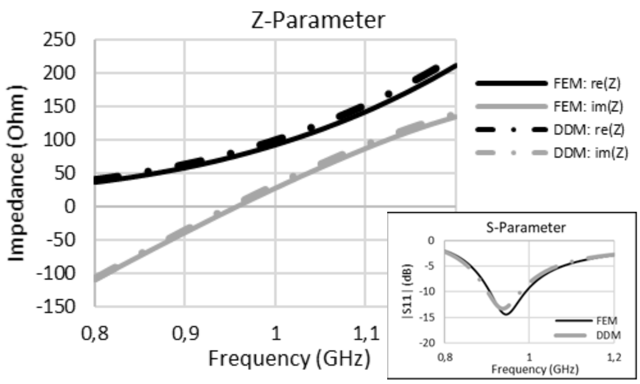

Fig. 4. Real and imaginary part of Z-parameter solved with FEM and DDM, and (inset) Magnitude of the reflection coefficient $|S_{11}|$, for a half-wave dipole over a finite PEC.

TABLE II. COMPUTATIONAL PERFORMANCE FOR A HALF-WAVE DIPOLE OVER A FINITE PEC

Method	*Unknowns*	*Adaptive Meshing (Time / Memory)*	*Frequency Sweep (Time / Memory)*
FEM	31 751	1 min 55 s / 2.14 GB	6 min 02 s / 28.3 GB
DDM	173 197	5 min 15 s / 7.34 GB	3 h 11 min / 7.34 GB

C. *Half-wave flat dipole over a mushroom-like AMC validation*

A half-wave flat dipole operating at 940 MHz (λ_0 = 319 mm) is designed on a FR4 substrate (ε_r = 4.4 and tan δ = 0.02). The substrate size is 150 x 15 x 0.8 mm³. The half-wave dipole is centered over a finite AMC at the height of $h_{radiator}$ = 17 mm ($\lambda_0/19$), Fig. 5. For DDM simulation, the radiator is sliced in three different regions, depending on the size of the AMC unit cell, Fig. 5(c). The AMC unit cell is a mushroom-like structure [14]: a metallic square patch over a FR4 substrate is linked to a ground plane through a central via. The substrate height of the unit cell is h_{cell} = 5.1 mm. The unit cell periodicity is p = 60 mm ($\lambda_0/5.3$) and the gap between each patch is g = 1 mm. One padding cell is implemented all around the metasurface.

Z and S-parameters are obtained with a minimum of 5 passes for both simulations, Fig. 6. The results in Table III are determined for 101 frequency points. A specific attention is paid to the mesh in order to approach the results of a full-wave simulation. The real and imaginary part of Z-parameter solved with DDM follow the same trend of those solved with FEM but with a frequency shift of 2%. As seen in both previous cases, even if HPC is oversized for this case of study, the memory consumption is reduced by 7 times during frequency sweep process with DDM, but with high cost in simulation time, 40 times higher than FEM simulation. This third case is also for validation only and it is not a practical use case.

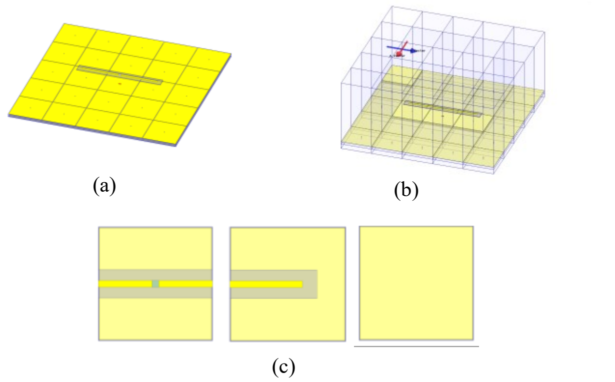

Fig. 5. Half-wave flat dipole over a finite mushroom–like AMC in HFSS. (a) Full-wave method. (b) DDM. (c) 3D Component unit cells: a feeding part over an AMC unit cell, an edge part of the dipole over an AMC unit cell and a single AMC unit cell.

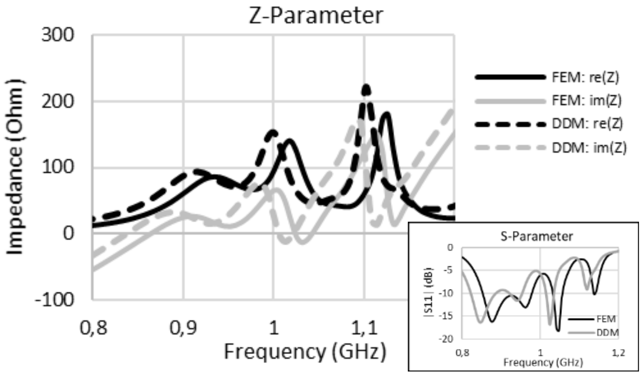

Fig. 6. Real and imaginary part of Z-parameter solved with FEM and DDM, and (inset) Magnitude of the reflection coefficient $|S_{11}|$, for a half-wave dipole over a finite mushroom-like AMC.

TABLE III. COMPUTATIONAL PERFORMANCE FOR A HALF-WAVE FLAT DIPOLE OVER A FINITE MUSHROOM-LIKE AMC

Method	*Unknowns*	*Adaptive Meshing (Time / Memory)*	*Frequency Sweep (Time / Memory)*
FEM	215 135	8 min 16 s / 13.61 GB	17 min 34 s / 141 GB
DDM	674 483	9 min 22 s / 19.27 GB	11 h 30 min / 19.44 GB

D. Half-wave flat dipole over a large complex AMC

The previous half-wave flat dipole is centered over a large complex AMC at the height of $h_{radiator}$ = 17 mm (λ_0/19). The unit cell layout is similar to [8] except the pattern here is a square patch and not a square spiral, Fig.7. The periodicity of the cell is p = 11.8 mm (λ_0/27) and the gap between each patch is g = 0.4 mm. The resistors value is R = 0.2 Ω and the capacitors value is C = 2.44 pF. In infinite array simulation, the AMC is designed to operate around 940 MHz. The size of the AMC is 19 x 9 unit cells. Seven padding cells are implemented in order to respect a distance around λ_0/4 between the edges of the antenna and the radiation boundaries.

For this antenna structure, the HPC setup used for DDM simulation is the same setup used during the validation step, for all the previous canonical models, with 40 cores where each core performs one task. This initial HPC setup does not work, in this case, for the full-wave simulation due to a lack of memory. A new parallel processing is configured for the FEM simulation to be run: 40 cores split in 10 cores per task and an interpolating frequency sweep. Computational statistics are available in Table IV.

Z and S-parameters, Fig. 8 are obtained with a minimum of 5 passes for both simulations. The real and imaginary part of Z-parameter solved with DDM follow the same trend of those solved with FEM but with still a frequency shift of 2%.

As the reflection coefficient of the model does not abruptly resonate, the choice of an interpolating frequency sweep was adapted to this case. 8 frequencies are solved for the interpolating frequency sweep. However, those results are obtained with a reconfiguration of the HPC parallel processing and it still needs substantial memory space to be performed: 76.02 GB at the adaptive meshing and 131.5 GB at the frequency sweep step, Table IV. Meanwhile, with the original HPC setup, the DDM simulation is completed with less than 10 GB of memory for more than 2 million unknowns at the meshing and frequency sweep steps, respectively 8.7 times and 13.4 times lower than FEM simulation. About the time consumption at the frequency sweep step, comparing on a like-for-like basis by considering only 8 points and not 75 points for the DDM simulation, the simulation time is 7 times higher than the FEM simulation (66 times higher on the actual basis). Nevertheless, the DDM is a time-consuming method, but this can be minimized by choosing platforms with both high speed CPU and moderated RAM capacity.

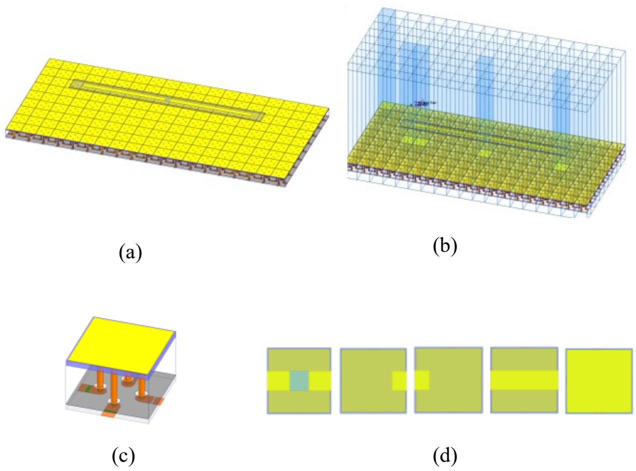

Fig. 7. Half-wave flat dipole over a large complex AMC in HFSS. (a) Full-wave method. (b) DDM. (c) Unit cell geometry of the AMC. (d) 3D Component unit cells: a feeding part over a AMC unit cell, two edge parts of the dipole over a AMC unit cell, a sleeve part over an AMC unit cell and a single AMC unit cell.

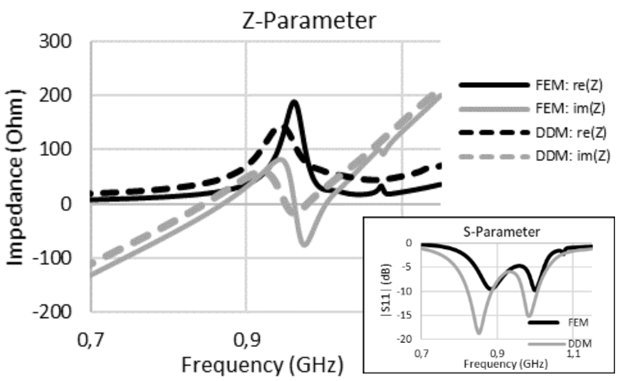

Fig. 8. Real and imaginary part of Z-parameter solved with FEM and DDM, and (inset) Magnitude of the reflection coefficient $|S_{11}|$, for a half-wave flat dipole over a large complex AMC.

TABLE IV. COMPUTATIONAL PERFORMANCE FOR A HALF-WAVE FLAT DIPOLE OVER A LARGE COMPLEX AMC

Method	***Setup***	***Unknowns***	***Adaptive Meshing (Time / Memory)***	***Frequency Sweep (Time / Memory)***
FEM	Interpolating, 501 points 10 cores/task	1 334 510	39 min 36 s / 76.02 GB	37 min 23 s / 131.5 GB
DDM	Discrete, 75 points 1 cores/task	2 553 140	30 min 48 s / 8.75 GB	40 h 49 min / 9.85 GB

V. CONCLUSION

FA-DDM for large complex low-profile metasurface-based antenna was investigated in this paper, with HPC for parallel processing. A validation step was performed as the technique is used for non-identical unit cells in the lattice array. Three canonical and simple structures were simulated: the half-wave dipole, the half-wave dipole over a PEC and the half-wave flat dipole over a mushroom-like AMC. In order to approach the results of a full-wave simulation, special attention is required in the meshing process. Then, a half-wave flat dipole over a large complex AMC were simulated with FA-DDM. As the full-wave required a reconfiguration of the HPC with more cores allocated per task to perform, the DDM simulation is completed with less than 10 GB of memory and with 2% errors between FEM and DDM. For all the studied cases, FA-DDM occurs to be a time-consuming technique. Nevertheless, FA-DDM can be an alternative solution to full-wave characterization if computer memory is limited.

ACKNOWLEDGMENT

The authors are grateful to Dr Amazir Moknache, senior field application engineer at Ansys, for his help on the settings for using FA-DDM in HFSS.

REFERENCES

[1] S. B. Glybovski, S. A. Tretyakov, P. A. Belov, Y. S. Kivshar, and C. R. Simovski, 'Metasurfaces: From microwaves to visible', *Physics Reports*, vol. 634, pp. 1–72, May 2016, doi: 10.1016/j.physrep.2016.04.004.

[2] O. Quevedo-Teruel *et al.*, 'Roadmap on metasurfaces', *J. Opt.*, vol. 21, no. 7, p. 073002, Jul. 2019, doi: 10.1088/2040-8986/ab161d.

[3] J. Wang *et al.*, 'Metantenna: When Metasurface Meets Antenna Again', *IEEE Trans. Antennas Propagat.*, vol. 68, no. 3, pp. 1332–1347, Mar. 2020, doi: 10.1109/TAP.2020.2969246.

[4] A. Bellion and M. Cable, 'A new wideband and compact High Impedance Surface', in *2012 15 International Symposium on Antenna Technology and Applied Electromagnetics*, Jun. 2012, pp. 1–5, doi: 10.1109/ANTEM.2012.6262322.

[5] N. Kristou, J.-F. Pintos, K. Mahdjoubi, 'Alternative Approach to Miniaturize an AMC Structure', *7th International Conference on Metamaterials, Photonic Crystals and Plasmonics (META),* Malaga, Spain, July 25-28, 2016.

[6] M. E. de Cos, F. Las Heras, and M. Franco, 'Design of Planar Artificial Magnetic Conductor Ground Plane Using Frequency-Selective Surfaces for Frequencies Below 1 GHz', *Antennas Wirel. Propag. Lett.*, vol. 8, pp. 951–954, 2009, doi: 10.1109/LAWP.2009.2029133.

[7] C. P. Scarborough, D. H. Werner, and D. E. Wolfe, 'Compact Low-Profile Tunable Metasurface-Enabled Antenna With Near-Arbitrary Polarization', *IEEE Trans. Antennas Propagat.*, vol. 64, no. 7, pp. 2775–2783, Jul. 2016, doi: 10.1109/TAP.2016.2562666.

[8] N. Kristou, J.-F. Pintos, K. Mahdjoubi, 'Miniaturized Tunable Artificial Magnetic Conductor for Low LTE Band', *IEEE Antennas and Propagation Society International Symposium (APS)*, San Diego (USA), July 9-14, 2017.

[9] E. Harper, C. Reistad, and A. Akyurtlu, 'Investigation of efficient simulation methods for finite large X-band arrays in HFSS', in *2017 International Applied Computational Electromagnetics Society Symposium - Italy (ACES)*, Florence, Mar. 2017, pp. 1–2, doi: 10.23919/ROPACES.2017.7916408.

[10] ANSYS. "HFSS 2020" [Software]. Available from: https://www.ansys.com/products/electronics/ansys-hfss

[11] Zuo, Z. Lin, J. Liu, D. Garcia-Donoro, Y. Zhang, and X. Zhao, 'A Fast Parallel Solution Technique for Large Periodic Structures Based on FEM-DDM', *Antennas Wirel. Propag. Lett.*, vol. 19, no. 10, pp. 1704–1708, Oct. 2020, doi: 10.1109/LAWP.2020.3014349.

[12] K. Zhao and M. Commens, 'A fast and efficient domain decomposition approach for finite antenna arrays', in *2013 IEEE MTT-S International Microwave Symposium Digest (MTT)*, Seattle, WA, USA, Jun. 2013, pp. 1–3, doi: 10.1109/MWSYM.2013.6697686.

[13] ANSYS, HFSS Help - Release 2020 R1 (User Guide). Canonsburg: ANSYS, 2020.

[14] D. Sievenpiper, Lijun Zhang, R. F. J. Broas, N. G. Alexopolous, and E. Yablonovitch, 'High-impedance electromagnetic surfaces with a forbidden frequency band', *IEEE Trans. Microwave Theory Techn.*, vol. 47, no. 11, pp. 2059–2074, Nov. 1999, doi: 10.1109/22.798001.